C_6F_6 and sym-$C_6F_3H_3$: Ab Initio and DFT Studies of Structure, Vibrations, and Inelastic Neutron Scattering Spectra

Dale A. Braden[†] **and Bruce S. Hudson***[,‡]

Department of Chemistry, University of Oregon, Eugene, Oregon 97403-1253, and Department of Chemistry, Syracuse University, Syracuse, New York 13244-4100

Received: July 26, 1999; In Final Form: November 2, 1999

The inelastic neutron scattering spectra of crystalline hexafluorobenzene (HFB) and 1,3,5-trifluorobenzene (TFB) are reported and compared to the results of calculations of the full spectral intensity based on density functional calculations (DFT). It is shown that several of the previous assignments of optically inactive fundamentals are incorrect, bringing the experimental picture into much better agreement with the calculated frequencies. For HFB the scattering is predominantly coherent, in contrast to the TFB case where hydrogen atom scattering predominates. There is generally good agreement between the calculated scattering intensities and the observed spectra. For TFB a comparison of the calculated and observed neutron spectra shows some significant differences attributed at least in part to hydrogen bonding in the crystal. The structures of these two molecules are discussed with reference to the reliability of the density functional methods and the effect of hydrogen bonding on the structure of TFB. It is argued that the CC bond length in HFB is shorter than for benzene consistent with similar effects for other π-electron systems.

Introduction

It is well established that ab initio and density functional treatments of molecular vibrations provide reliable frequencies. In many cases the disagreement between theory and experiment can be ascribed to the use of the harmonic approximation in comparison with an experimental frequency that exhibits anharmonicity as is particularly the case for C−H stretch motions. Another generalization is that Hartree−Fock (HF) calculations tend to provide results that are too high by about 10% relative to the experiment.[1] DFT methods tend to be within a few percent of experiment except for the C−H stretches.[1]

There have been fewer comparisons between such ab initio and DFT methods for the calculation of vibrational frequencies for fluorocarbons.[2−8] In a recent study of hexafluorobutadiene[2] we found that DFT methods produce vibrational frequencies accurate to an RMS value of about 27 cm^{-1}. Similar results are found for tetrafluoromethane, tetrafluoroethylene (unpublished), and, as presented here, 1,3,5-trifluorobenzene (TFB). A recent paper compares the results of high-level calculations with the vibrational spectra of CF_4 and C_2F_4.[3] In the case of hexafluorobenzene (HFB) the RMS deviation with a standard DFT method is about the same or even less than for these other cases. However, it was noticed that for large basis set DFT calculations the RMS error for the eleven IR or Raman allowed vibrations was much smaller (ca. 8 cm^{-1}) than for the nine vibrations that are forbidden in these optical spectroscopies. In these cases overtones and combinations were often used to deduce fundamental frequencies. For these nine silent modes an RMS value of 40−50 cm^{-1} was found. This fact alone suggests an error in one or more of the assignments of these fundamental frequencies, because there is no correlation between the accuracy of the calculated frequency of a mode and whether that mode is active or forbidden. Furthermore, there were four vibrations for which it was found that the assigned fundamental frequencies were actually higher than the values calculated in the HF approximation. For example, the B_{2g} vibration ν_5, calculated to be at 204 cm^{-1} with a HF/6-311+G* calculation, had been assigned as being at 248[9] or 243 cm^{-1}.[10] This discrepancy has been previously noted.[11] This pattern of large discrepancies between theory and experiment for modes that are forbidden in optical spectroscopies suggested that an inelastic neutron scattering (INS) study would be in order. This method of vibrational spectroscopy is not restricted by selection rules. The results of that experimental study, a revision of the assignments of the vibrations of hexafluorobenzene, and a simulation of the entire coherent inelastic neutron scattering spectrum are reported here.

Intermolecular interactions between fluorobenzenes are the subject of a recent X-ray structure investigation.[12] This study shows that fluorobenzenes such as TFB have lattice arrangements that are very similar to the corresponding azines and are thus best interpreted in terms of CH···F hydrogen bonding. The inelastic neutron scattering spectrum of 1,3,5-trifluorobenzene was also determined and compared with the result computed from a large basis set density functional calculation. In this case the INS spectrum is dominated by the contribution of H atom motion to a particular mode. The maximum possible intensity is obtained when a vibration is 100% H atom motion. This upper limit to the possible intensity reduces some of the arbitrariness in the adjustment of the relative scaling of computed and observed spectra. In this case the intensity comparison reveals intermolecular interactions in the solid that appear to restrict the molecular motions as expected for hydrogen bonding.

There have been several comparisons of the minimum energy geometries of fluorocarbons obtained with modern theoretical methods and experiment.[2,3,13−15] The DFT calculations with the largest basis set reproduce the ground state rotational constant for both HFB and TFB, but the geometries differ slightly from the GED structures. The differences are discussed. A comparison

[†] University of Oregon. E-mail: genghis@darkwing.uoregon.edu.
[‡] Syracuse University. E-mail: bshudson@syr.edu.

10.1021/jp992580w CCC: $19.00
Published on Web 12/21/1999

TABLE 1: Calculated and Observed Vibrational Frequencies for Hexafluorobenzene

calculation ⇒ experiment ↓				A HF	B HF X 0.9	C MP2	D DFT B3LYP	E DFT B3P W91	F DFT B3LYP	G DFT B3LYP
		Raman & IR (cm^{-1})	INS cm^{-1}	6−311 +G*		6−31 +G(d′)	6−311 +G*	6−311 +G*	6−311 +G(3df)	aug-cc-pVTZ
Raman or IR Active Modes:										
ν_{11}	A_{2u}	210	230	247	222	220	216	219	219	212
ν_9	E_{2g}	267	269	296	266	267	271	269	275	270
ν_{20}	E_{1u}	313	315	345	310	315	316	318	320	315
ν_{10}	E_{1g}	365	369	442	398	377	374	378	382	369
ν_8	E_{2g}	440	442	484	436	444	446	446	446	447
ν_2	A_{1g}	556	558	608	547	560	561	567	565	564
ν_{19}	E_{1u}	1019		1107	996	1009	1009	1023	1023	1016
ν_7	E_{2g}	1162		1281	1152	1162	1161	1179	1169	1168
ν_1	A_{1g}	1493		1665	1498	1525	1503	1526	1509	1507
ν_{18}	E_{1u}	1533		1701	1531	1558	1539	1559	1549	1540
ν_6	E_{2g}	1656		1848	1663	1697	1671	1689	1671	1667
		RMSΔ (IR & Raman)		109	14	18	8	18	11	7
		RMSΔ (with INS)		108	13	18	8	18	11	9
Raman and IR Inactive Modes:										
ν_{17}	E_{2u}	137		152	137	135	136	136	139	137
ν_5	B_{2g}	**248**	205	204	183	108	184	185	187	184
ν_{15}	B_{2u}	**201**	278	304	273	276	279	278	285	279
ν_{13}	B_{1u}	**645**	600	642	578	600	596	599	558	602
ν_4	B_{2g}	**719**	719	718	646	296	651	607	779	745
ν_{16}	E_{2u}	**645**	645	738	664	627	663	661	690	666
ν_3	A_{2g}	**763**	788	865	778	773	792	796	811	793
ν_{14}	B_{2u}	**1252**		1184	1065	1454	1306	1333	1304	1298
ν_{12}	B_{1u}	1330		1467	1320	1320	1323	1338	1246	1332
		RMSΔ (IR & Raman)		78	78	166	49	60	63	42
		RMSΔ (with INS)		67	68	160	30	47	45	20

of the CF bond lengths in TFB reveals what appears to be significant elongation of the CF bonds in the solid state relative to the isolated molecule.

Experimental Methods

The neutron scattering spectra were obtained with the TOSCA[16] instrument of the ISIS Spallation Neutron Source at the Rutherford Appleton Laboratory. At the time of these experiments TOSCA had only the backscattering bank of detectors installed and had not yet been moved radially outward for improved resolution relative to TFXA. Experiments on high molecular mass samples (where the line width is instrument limited) indicate that TOSCA in the configuration used has a resolution that is slightly better than TFXA (e.g., ca. 6 to 12 cm^{-1} over the range of the spectra shown in this paper). Data were acquired over a frequency range of 16−4000 cm^{-1}.

The two samples investigated are liquids at room temperature. They were contained in aluminum sample cells with indium gaskets. The samples were held at about 10 K in a cryostat. The sample mass was 10 g for HFB, 1 g for TFB.

Computational Methods

Geometry optimization and vibrational analysis calculations were carried out using the *Gaussian 94* and *Gaussian 98* programs[17] primarily at NCSA in Illinois. The B3LYP and B3PW91 hybrid density functionals, as implemented in the *Gaussian* programs, were used for the DFT calculations. A variety of basis sets were used as indicated in Tables 1 and 2. The geometry of HFB was constrained to D_{6h} symmetry for the geometry optimizations, and TFB was constrained to D_{3h} symmetry.

In the limit of low temperature only the zero point level is populated. In this case for the TFB spectra where the incoherent scattering of hydrogen dominates, the quantity relevant to the neutron scattering intensity is the sum of the squares of the H atom components in the (normalized) eigenvectors defining each normal mode coordinate, i.e., $\Sigma_i(C_{(Hi)})^2$.[18] For HFB where the scattering is predominantly coherent the relevant quantity for each normal mode is the sum over all pairs of atoms *ij* of the quantity $b_i b_j(\mathbf{Q}\cdot\mathbf{C}_i)(\mathbf{C}_j\cdot\mathbf{Q})\exp(i\mathbf{Q}\cdot\mathbf{R}_{ij})$ where b_i and b_j are the atomic scattering lengths ($4\pi b^2$ is the cross section), **Q** is the momentum transfer vector, $\mathbf{C}_i$ and $\mathbf{C}_j$ are the vector components of the motion of atom *i* (or *j*) in the mode in question, and $\mathbf{R}_{ij}$ is the vector between the equilibrium position of atom *i* and atom *j*.[19] Since **Q** is defined in the laboratory frame and the **C**s and $\mathbf{R}_{ij}$ are defined in the molecular frame, it is necessary to perform an orientation average before comparison with experiment. In this case this involves a two-dimensional integration which was performed using Mathematica. The necessary equivalence of the intensities calculated for two components of a degenerate pair was used as a test of the adequacy of the orientation averaging procedure.

Results

The determination of the INS spectrum of hexafluorobenzene was motivated by the data shown in Table 1. It was found that thirteen of the 20 unique vibrational frequencies of this molecule were well reproduced by B3LYP density functional calculations using the aug-cc-pVTZ basis set (RMSΔ of 7 cm^{-1}). However, seven of the modes whose frequencies had been deduced on the basis of IR and Raman experiments, shown in Table 1 in bold, had much larger deviations than expected on the basis of other comparisons with experiment (RMSΔ of 55 cm^{-1}). Four of these seven modes have frequencies that are higher than those calculated at the HF level, which is known to *overestimate* harmonic frequencies by about 10%.[1] It was noticed that all of these discrepant modes were inactive in both Raman and IR spectroscopies. This observation suggested that it was the interpretation of the experimental data that was in error.

TABLE 2: Comparison of Calculated and Observed Optical and Inelastic Neutron Scattering Frequencies for 1,3,5-trifluorobenzene

						B3LYP			
		experiment		B3PW91				aug-cc-pVTZ	
vib. no.	sym.	IR & Raman	INS	6−31 ++g*	6−311 +g*	6−31 ++g**	6−311 +g*	freq	$\Sigma_i(C_{(H)i})^2$
ν_{17}	A_2''	207		208	209	207	208	209	0.02
ν_{20}	E''	246	**260**	250	249	250	250	251	1.34
ν_{14}	E'	328	**327**	326	327	324	324	326	0.31
ν_{13}	E'	504	**503**	505	507	507	510	510	0.92
ν_7	A_2'	564	**551**	555	557	553	555	558	0.74
ν_4	A_1'	580		582	582	577	577	581	0.00
ν_{19}	E''	598	**594**	605	608	601	604	610	1.47
ν_{16}	A_2''	663	**665**	669	668	667	667	683	0.91
ν_{18}	E''	792	**852**	847	843	850	845	857	1.91
ν_{15}	A_2''	847	**852**	847	845	851	850	876	0.92
ν_{12}	E'	996	**997**	1018	1017	1010	1008	1010	1.67
ν_3	A_1'	1012		1023	1021	1023	1022	1026	0.52
ν_{11}	E'	1129	**1124**	1148	1145	1140	1137	1136	1.86
ν_6	A_2'	1165	**1206**	1227	1230	1232	1234	1226	0.97
ν_5	A_2'	1294		1387	1377	1365	1353	1348	0.54
ν_2	A_1'	1363		1388	1379	1367	1359	1363	0.02
ν_{10}	E'	1475		1511	1508	1501	1498	1496	1.42
ν_9	E'	1622		1676	1673	1661	1656	1652	0.76
ν_1	A_1'	3076		3256	3233	3244	3224	3224	0.99
ν_8	E'	3116		3257	3234	3245	3224	3225	1.98
	RMS error (w/o CH str) (cm^{-1})		IR & Raman	35	32	29	27	28	
			with INS	29	27	22	19	19	

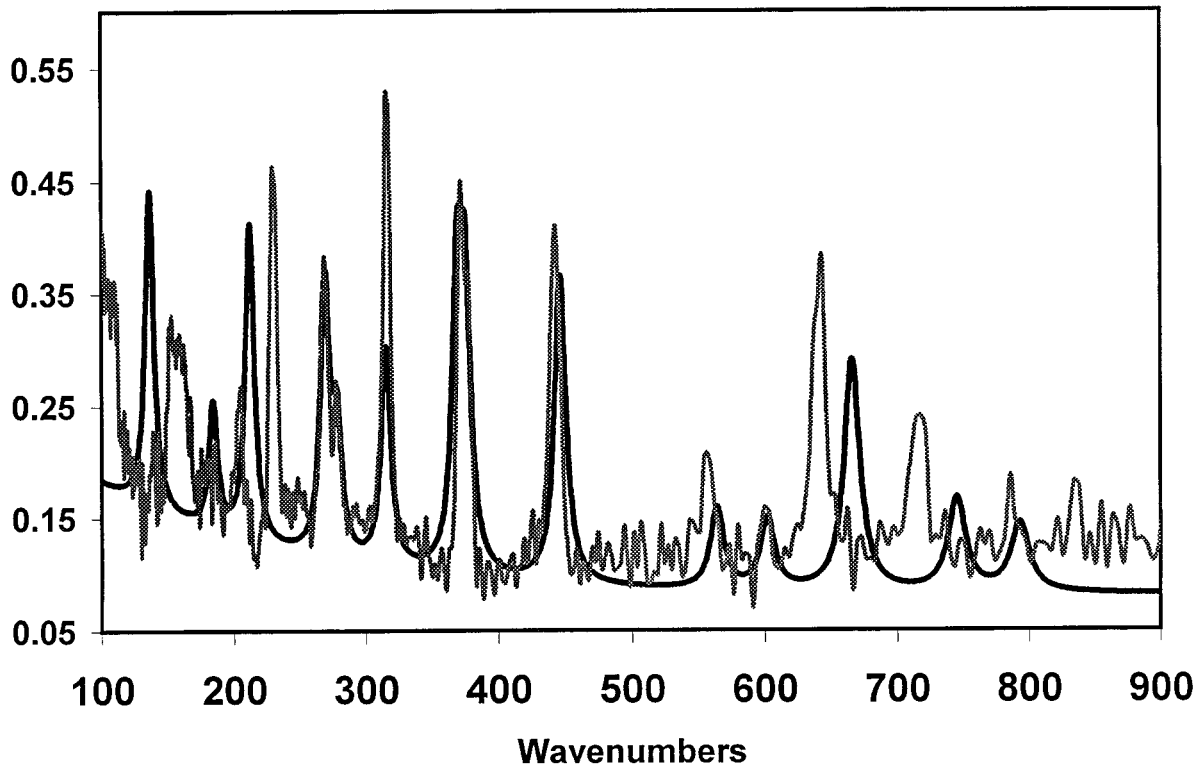

Figure 1. Inelastic neutron scattering spectrum of hexafluorobenzene compared to a simulated spectrum based on the methods and results of column G of Table 1 and the corresponding normal mode eigenvectors.

Examination of a variety of basis sets and calculation methods did not result in any case of significantly reduced discrepancy. It did reveal, however, that several of the normal vibrational frequencies of hexafluorobenzene appear to be quite sensitive to the method and basis set used. The MP2 calculation, in particular, provides values that are in some cases widely divergent from the values of all other methods and from experiment. The case of ν_4 is most extreme in this regard. Here the MP2 value is less than half the observed value which is confirmed by the INS studies. The DFT B3LYP method with the aug-cc-pVTZ basis set clearly provides the best agreement with experiment for the Raman/IR active modes. For the inactive modes, however, this basis set, while providing the lowest RMS deviation, is not significantly better than the other four DFT calculations using other basis sets and is considerably larger than seen for other molecules.

The INS spectrum of HFB is shown in Figure 1 where it is compared with the spectrum calculated on the basis of the DFT/B3LYP/aug-cc-pVTZ basis. The agreement between calculated and observed spectral frequencies and intensities is reasonably good in the intermediate region from 250 to 500 cm^{-1} but degrades at both higher and lower frequencies. However, even

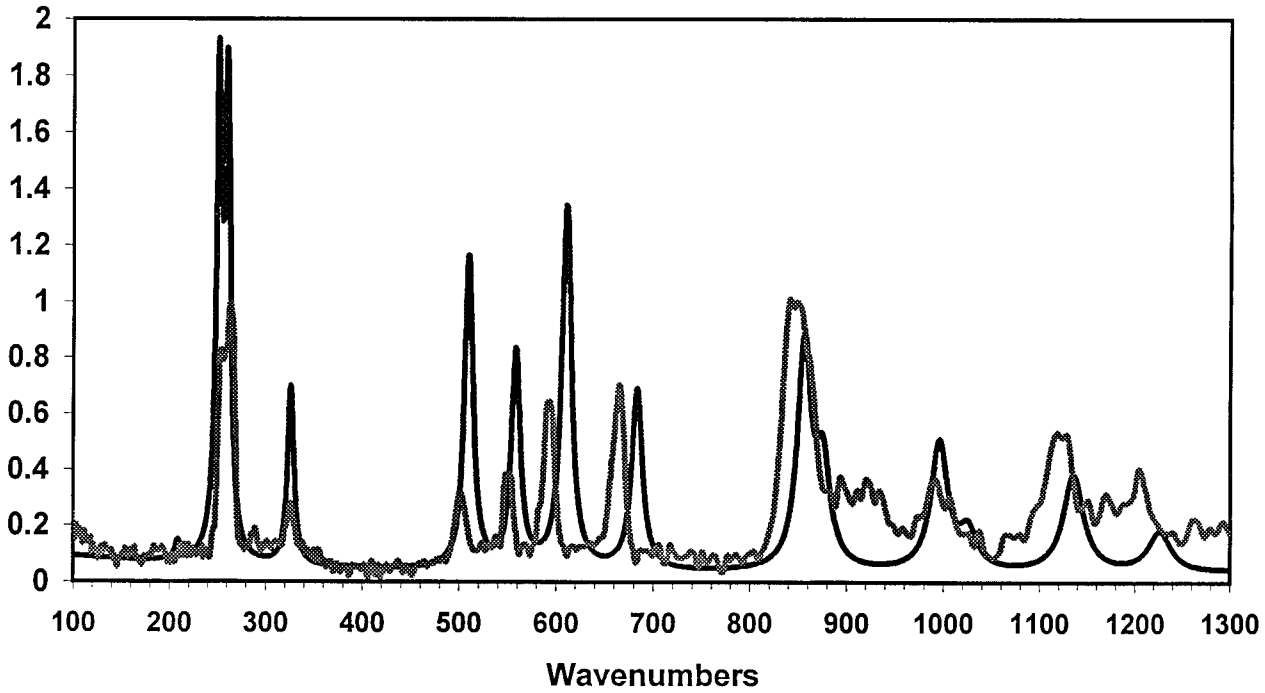

Figure 2. Inelastic neutron scattering spectrum of 1,3,5-trifluorobenzene compared to a simulated spectrum based on the B3LYP/aug-cc-pVTZ results of the last two columns of Table 2. The lowest frequency E'' mode ν_{20} at 251 cm^{-1} has been split into components at 251 and 260 cm^{-1} in order to match the observed site group splitting.

in these marginal regions it is possible to use the neutron intensities to confirm the assignment of the observed features. In this way the transitions can be identified without ambiguity.

The frequencies of HFB deduced from the INS spectrum are listed in Table 1. Seven of the nine inactive frequencies of HFB are easily seen in the INS spectrum. Two of the modes (4 and 16) are seen at values inferred from the optical experiments. However, four (modes 3, 5, 13, and 15) are seen at values much closer to the calculated values (RMSΔ for these four modes of 5.5 cm^{-1}). This confirms the attribution of about 2/3 of the discrepancy between theory and experiment to incorrect assignment of the fundamental frequencies on the basis of the optical spectra. In many cases the change in the value of the frequency is very large, especially if considered on a percentage basis. However, the comparison of intensities shown in Figure 1 confirms the validity of these major revisions in assignment. The RMS deviation based on these INS values plus IR or Raman values where INS values are not observed is given below the optical values in Table 1. With the revised assignment there is enhanced discrimination of the computational methods. The aug-cc-pVTZ basis appears to be in significantly better agreement for both optically allowed and forbidden sets of vibrations than the other basis sets. Furthermore, the magnitude of the residual deviation is in line with that observed in other cases.

Most of the error in the MP2 results is for ν_4, ν_5, and ν_{14}, where the calculated frequencies differ greatly from both the experimental values and the values calculated by DFT. Note, however, that ν_{14} was too high in frequency to be observable in the INS spectrum, and its experimental assignment is based on observed combination bands in the Raman spectra [ref 9 and refs therein]. Modes ν_4 and ν_5 are both of B_{2g} symmetry and correspond to out-of-plane motion of the carbon atoms and fluorine atoms, respectively. For ν_5, the results of the (scaled) Hartree−Fock and DFT calculations using all basis sets are in very close agreement, and they all agree with the observed INS frequency for this mode. Only the MP2 value is widely different. For ν_4, there is a strong dependence on both method and basis set; even the two hybrid DFT functionals yield significantly different values using the same basis. This sensitivity is also evident in the case of TFB. The two modes which show the strongest dependence on basis set for TFB are ν_{16} and ν_{15} (Table 2). These modes are of A_2'' symmetry, which corresponds to B_{2g} symmetry in the D_{6h} point group of HFB. Both modes correspond to out-of-plane motion of the hydrogen atoms, in phase or out of phase, respectively, with their attached carbons. The frequencies calculated for these modes increase by 16 and 26 cm^{-1}, respectively, when the basis is changed from 6-311+G* to aug-cc-pVTZ. Clearly the calculated frequencies associated with these modes are extremely dependent on the treatment of electron correlation.

We turn now to the case of TFB. Table 2 presents the comparison between the results of five B3LYP DFT calculations with the assignment of IR and Raman spectra. The experimental results are for vapor phase for all optically allowed transitions (Raman: A_1', E', E''; IR: E', A_2'')[20] and are for solutions in CS_2 or CCl_4 for the forbidden transitions (A_2').[21] Four of these five basis sets give mean square frequency differences similar to each other and to what is expected from comparisons for other molecules. We pick the aug-cc-pVTZ for discussion. The largest percentage discrepancy between theory and this calculation is for ν_{18}, an E'' mode assigned as being at 792 cm^{-1} but calculated by all methods at 830−860 cm^{-1}. On the basis of its square hydrogen amplitude this mode is expected to give rise to a strong transition in the INS spectrum. Note that the next higher frequency mode, ν_{15} of A_2'' symmetry, has been assigned at 847 cm^{-1} and is thus in the region where ν_{18} is expected.

In comparing the calculated spectrum with that observed, the overall scaling factor can be adjusted arbitrarily. In the spectrum shown in Figure 2 this scale factor has been chosen so as to match the height of the peak at 663 cm^{-1} due to the A_2'' mode ν_{16}. With this scaling the total intensity distribution at higher frequency is well reproduced. However, the lower frequency peaks are then too large by as much as a factor of 2. It is, of course, possible to use a scaling that results in better agreement

TABLE 3: Bond Lengths (Å) and Calculated Equilibrium Rotational Constants (cm^{-1}) for Hexafluorobenzene

			calculation					
	experiment		HF	MP2	DFT B3LYP	DFT B3PW91	DFT B3LYP	DFT B3LYP
	X-ray[a]	GED[b]	6-311+G*	6-31+G(d′)	6-311+G*	6-311+G*	6−311 +G(3df)	aug-cc-pVTZ
R(CC)	1.36 ± 0.02	1.394 ± 0.007	1.3772	1.3975	1.3907	1.3891	1.3883	1.3887
R(CF)	1.32 ± 0.017	1.327 ± 0.007	1.3080	1.3355	1.3336	1.3275	1.3294	1.3315
B_e[c]			0.0351778	0.0339868	0.0342190	0.0343962	0.0343806	0.0343218

[a] The X-ray bond lengths are from ref 32. [b] The GED bond lengths are from ref 28. [c] The experimental value of B_0 is 0.0343165 cm^{-1}.[22]

TABLE 4: Bond Lengths (Å) and Calculated Equilibrium Rotational Constants (cm^{-1}) for 1,3,5-trifluorobenzene

			calculation				
	experiment		DFT B3PW91	DFT B3LYP	DFT B3PW91	DFT B3LYP	DFT B3LYP
	X-ray[a]	GED[b]	6-31++G**	6-31++G**	6-311+G*	6-311+G*	aug-cc-pVTZ
R(CC)	1.381 ± 0.003	1.402 ± 0.006	1.3890	1.3909	1.3855	1.3873	1.3841
R(CF)	1.356 ± 0.003	1.305 ± 0.006	1.3461	1.3531	1.3415	1.3486	1.3460
B_e[c]			0.0584769	0.0581774	0.0587525	0.0584550	0.0587059

[a] The X-ray bond lengths are from ref 12 but are then averaged. [b] The GED bond lengths are from ref 33. [c] The experimental value of B_0 is 0.0586517 cm^{-1}.[22] No B_e values were calculated for the XRD or GED structures because more geometrical information is required.

in the low frequency region at the expense of the higher modes. This might be an appropriate approach if the differences in intensity were thought of as being due to error that is randomly distributed. In this case the result would be an intensity distribution that is too low from 650 cm^{-1} upward, specifically at the peak for ν_{16} and the combined peak ν_{18} and ν_{15}. One would then have to argue that some improvement in the molecular force field would improve on this degree of agreement by increasing the intensity of these peaks. However, the calculated intensity of all three of these vibrations is within 10% of the maximum possible value since the sum of the squares of the hydrogen atom components for each of them is above 0.9 with a maximum value of unity. The inclusion of a large Debye−Waller factor causes the calculated intensity distribution to be even more skewed toward low frequency. We must, then, look elsewhere for an explanation of this discrepancy.

Discussion

Geometries. Tables 3 and 4 give the calculated and experimental values for the CF and CC bond lengths in HFB and TFB, respectively. The rotational constants determined from pure rotational Raman scattering[22] are also given and compared with the value calculated for this quantity from the bond lengths obtained by geometry optimization for each method. D_{6h} symmetry applies for HFB and D_{3h} for TFB.

The rotational constant for HFB was determined from pure rotational Raman scattering at a temperature of 20 °C, which means that several vibrational levels were populated.[22] However, Schlupf and Weber reported that the Raman lines were very sharp, which indicated that the geometries of the vibrationally excited states were essentially the same as those of the ground state. They therefore reported the rotational constant as B_0, which refers to the moment of inertia for rotation of the symmetry axis for the molecule in its zero point level ($\nu = 0$). The quantity that can be directly obtained from an ab initio calculation is B_e, which corresponds to the geometry at the minimum of the potential energy surface. B_e and B_0 differ because of the effects of zero-point motion, the Coriolis interaction, and anharmonicity of the vibrations.[23] The sharpness of the Raman lines indicates that the effects of anharmonicity on the rotational constant are negligible. Since we have a description of the motion of the nuclei from the (harmonic) normal mode calculations we can adjust B_e to account for the effects of zero-point motion and Coriolis coupling. The corrections were calculated using the ASYM40 program[24] and the normal mode data from the B3LYP/aug-cc-pVTZ calculations. For HFB, $B_e = 0.0343218$ cm^{-1} and B_0(calcd) = 0.0343214 cm^{-1}. For TFB, $B_e = 0.0587059$ cm^{-1} and B_0(calcd) = 0.0587174 cm^{-1}. The correction in the case of HFB is negligible.

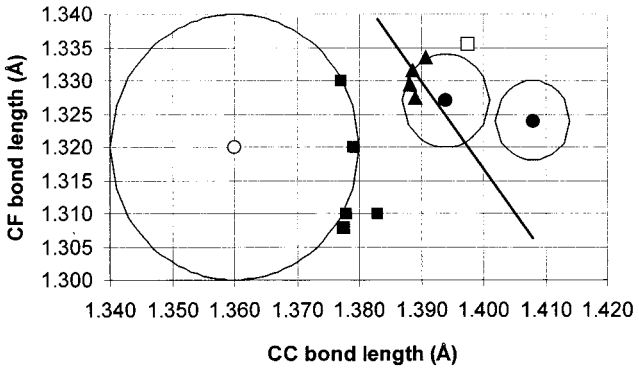

Figure 3. Plot of the experimental and calculated CF bond lengths vs the CC bond lengths for C_6F_6. The black squares are from Hartree−Fock calculations, including three from ref 11. The open square is for the MP2 calculation and the triangles are for the DFT calculations. The open circle is the XRD geometry[32] and the two solid circles are the GED geometries,[28,33] all surrounded by circles representing the associated error bounds. The line corresponds to those pairs of values that are consistent with the observed value of B_0.[22]

One of the surprising observations is that the value of B_0 for HFB calculated with B3LYP/aug-cc-pVTZ differs from the experimental B_0 by only 4.9×10^{-6} cm^{-1} (B_0(exptl) = 0.0343165 cm^{-1}).[22] This is very good agreement: an increase in the CC bond length of only 0.00018 Å or in the CF bond length of 0.00024 Å would give exact agreement. The other methods or basis sets do not provide anything like this degree of precision. B3LYP/aug-cc-pVTZ also yields the best value of B_0 for TFB, although the discrepancy is larger in this case. It appears that the B3LYP/aug-cc-pVTZ method may be particularly well suited to the computational treatment of fluorocarbons, but further tests are necessary.

It is of interest to know whether perfluorination of the benzene ring causes a shortening of the CC bonds. There have been three experimental structure determinations of HFB, but they disagree significantly in the values for the bond lengths. Figure 3 shows the various calculated CC and CF bond lengths for HFB in a plot of the R(CF) vs R(CC) plane. Given the D_{6h} symmetry of this molecule, the molecular geometry is specified by a point

in this plane. The three experimental geometries are also shown with their stated error limits indicated by large circles. The diagonal line in Figure 3 is the set of molecular geometries for HFB, averaged over zero-point motion, that are consistent with the measured value of B_0. The width of the line is larger than that implied by the experimental precision in this number. The GED studies and the rotational Raman study were both carried out at room temperature. The sharpness of the Raman lines indicates that the vibrationally excited geometries of HFB at room temperature differ little from the ground state geometry.[22] Vibrational motion and centrifugal distortion both lead to increases in average bond lengths, so any corrections to the GED geometries must be to decrease the bond distances. Corrections for zero-point harmonic motion and centrifugal distortion at 287 K[28] were estimated with the ASYM40 program using the normal mode data from the B3LYP/aug-cc-pVTZ calculation, and amounted to 0.0034 Å for CC and 0.0067 Å for CF. These values are within the stated experimental error bounds. Because of the coincidence of the DFT geometries, the GED geometry of ref 28, and the B_0 line in Figure 3, we conclude that the most probable bond lengths in HFB are very close to 1.390 Å for CC and 1.330 Å for CF.

The CC bond length of 1.390 Å is significantly shorter than the value of R(CC) = 1.397 Å for benzene.[25] This was not clear from previous studies and is of interest since it relates to the balance between the weakening of π-bonding and the strengthening of σ-bonding by fluorine substitution. Perfluorination is known to cause a shortening of the C=C bond in tetrafluoroethylene relative to that in ethylene.[26] Bent's rule[27] provides a possible explanation for this. The electronegativity of F draws more p-character from the C orbitals which leaves more s-character in the bonds between the carbons. Because s-orbitals are more contracted than p-orbitals, the CC bonds shorten. This explanation may also apply for HFB, but because the CCC and FCC bond angles are constrained by symmetry to be 120°, the CC bonds should be "bent", i.e., the bonding electron density does not lie along the CC line.

A reviewer has noted that the CF and CC bond lengths in HFB are very similar, and that if they are not resolved in the radial distribution function of the GED experiment then their values may be unreliable. However, in general the radial distribution function has peaks for all intramolecular distances, and many of these are often well-resolved. Because of its high symmetry, the geometry of HFB is specifiable with only two parameters. Thus the entire radial distribution function (or scattering intensity curve) of HFB must be fit with only two geometrical parameters,[28] and so the similarity in CF and CC bond lengths is not a problem.

The structural parameters for TFB are given in Table 4 and the corresponding plot of R(CF) vs R(CC) for TFB is shown in Figure 4. In this case the CH bond length and one of the CCC angles is required in addition to the CF and CC bond lengths to determine the rotational constant. However, the CF and CC bond lengths are by far the most important in determining the moments of inertia, and hence the rotational constant, so it is justifiable to characterize the geometry by a two-dimensional plot. Again, the B3LYP/aug-cc-pVTZ calculation results in a value of B_0 for TFB (0.0587174 cm^{-1} after corrections for zero-point motion and Coriolis effects) that is closest to the experimental value (B_0 = 0.0586517 cm^{-1}), but the difference in this case is 131 times the standard deviation of the experimental number and is thus statistically significant. If the CF bond length is lengthened by 0.0017 Å then there is agreement with the experimental value of B_0. One could, of course, make a slightly smaller expansion of the CC bond length (0.0010 Å) to obtain the same result.

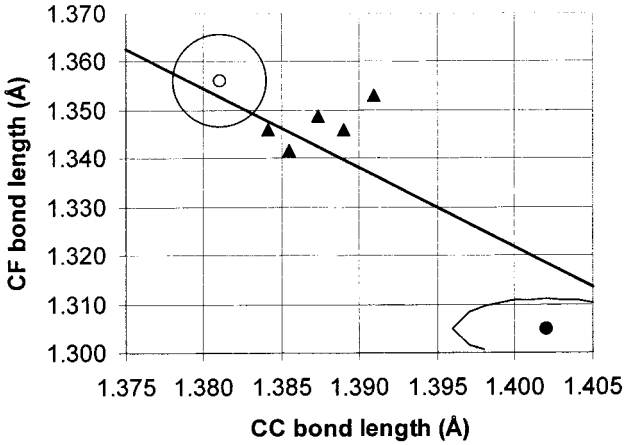

Figure 4. Plot of the experimental and calculated CF bond lengths vs the CC bond lengths for 1,3,5-trifluorobenzene. The triangles are for the DFT calculations. The open circle is the XRD geometry[12] and the solid circle is the GED geometry,[33] both surrounded by circles representing the associated error bounds. The line corresponds to those pairs of values that are consistent with the observed value of B_0.[22]

The DFT geometries are close to the B_0 line and to the XRD structure. Following the argument used with Figure 3 and HFB, we conclude that the most probable values for the CC and CF bond lengths are close to 1.383 and 1.350 Å, respectively. In comparison to the geometry for HFB, TFB has significantly longer CF bonds. This is reminiscent of the behavior of fluoromethanes where the CF bond length decreases in the series CH_3F, CH_2F_2, CHF_3, CF_4.[29] The CC bond length is certainly shorter than that in benzene, and somewhat shorter than that in HFB. The lengthening of the CF bonds in solid TFB could also be due to C−H···F hydrogen bonding. This is in agreement with a recent discussion of hydrogen bonding in such crystals based on the observed packing arrangements.[12] The magnitude of the effect based on our results is about the same as that observed for peptide hydrogen bonding.[30] We propose that this C−H···F hydrogen bonding not only deforms the molecule but also restricts the amplitude of the low-frequency motions as reflected in the intensities of the low-frequency modes (Figure 2).

Vibrations. The IR and Raman vibrational frequencies reported in Table 1 for hexafluorobenzene are from gas phase determinations.[9] The values for the inactive modes are inferred from combination bands and the use of band contours to determine symmetry type. The effect of the solid environment on the vibrational frequencies in this case can be established by comparing these gas-phase results with the results of an infrared study of the crystal at 77 K.[10] The largest effects are for ν_{11} and ν_{13}. The A_{2u} mode ν_{11} found in the gas phase at 210 cm^{-1} is seen as a pair of peaks at 226 and 229 cm^{-1} in the IR spectrum of the solid (and 230 in the INS spectrum). The B_{2u} mode ν_{13}, reported at 645 cm^{-1} in the vapor is assigned at 604 in the solid and seen at 600 in the INS spectrum. This change is probably a reassignment rather than a shift. The other shifts are smaller and do not appear to appreciably explain the residual discrepancies between the calculated and experimental values. For example, the large E_{2u} peak (ν_{16}) observed at 644 cm^{-1} in the INS spectrum, calculated to be at 666 cm-1 with the aug-cc-pVTZ basis is observed at 642 cm^{-1} in the IR spectrum of the solid and is inferred to be at 645 cm^{-1} from the vapor data. We therefore attribute the residual 20 cm^{-1} RMS deviation of the observed and calculated frequencies to remaining correlation

and basis set effects which, in some cases, happen to be in the opposite direction to the effects of anharmonicity and intermolecular interactions rather than in the same direction.

The assignment of the vibrations of HFB by Green and Harrison (G&H)[9] derived largely from the original work of Steele and Whiffen (S&W)[31] with a few significant reassignments and the use of new vapor phase data. The assignments by Laposa and Montgomery (L&M)[10] of the vibrations in the solid were based, when possible, on observations of peaks in the solid at positions previously assigned for fundamentals of the vapor or liquid. No mention was made by L&M of previous arguments indicating alternative possible assignments given by S&W, and the earlier work of G&H was not cited. The value of 137 cm^{-1} of G&H was chosen to provide agreement with gas-phase entropy data. On the basis of all of the ab initio and DFT calculations we concur on this assignment. The assignment of the B_{2g} symmetry mode ν_5 by G&H was retained from S&W and was based on the liquid-state value of 495 cm^{-1} in the Raman spectrum "taken as $2\nu_5$ "[9] (by S&W) "so the value 248 cm^{-1} must relate to that state".[9] The assignment of the B_{2u} symmetry mode ν_{15} at 201 cm^{-1} by G&H was based on the same argument used by S&W: an IR band at 1365 cm^{-1} (1363 cm^{-1} in G&H) has an E_{1u} contour. This implies, for example, $E_{2g} + B_{2u}$ (1162 + 201 cm^{-1}) or $B_{2g} + E_{2u}$ for the combination. The former was chosen by S&W as "more likely" apparently because it resulted in a value of ν_{15} in close agreement with the prediction of a normal mode calculation. However, the alternative noted by S&W of $\nu_4 + \nu_{16} = 719 + 645 = 1364$ cm^{-1} yields the same overall symmetry. This alternative assignment for the observed band at 1363 cm^{-1} allows the frequencies for ν_5 and ν_{15} to be switched, bringing them into much better agreement with the calculated values.

The assignments of ν_{13} and ν_{16} of B_{1u} and E_{2u} symmetry, respectively, will be discussed together. They were both assigned as being at 645 cm^{-1} by G&H. ν_{16} was originally assigned by S&W as being at 595 cm^{-1} based on observed Q-branches of combinations with E_{2g} modes. There is a mode seen in the IR of the solid at 604 cm^{-1}. We concur with G&H in the revision (on the basis of values for other fluorobenzenes) of the value of ν_{16} from ca. 600 cm^{-1} to 645 cm^{-1}. We then return to the data used to assign the B_{1u} mode ν_{13} as being at 645 cm^{-1}. This was based on the assignment by S&W of a "medium band" at 1086 cm^{-1} that "appears to have perpendicular band contour" to 443 (ν_8, E_{2g}) + 643 (ν_{13}, B_{1u}). This feature could, however, be due to ν_{20} (E_{1u}) at 313 cm^{-1} + ν_3 (A_{2g}) at 788 cm^{-1}. This assignment is made more plausible by our upward revision of the value for ν_3 from the previous value of 763 cm^{-1}. The reassignment of this combination band eliminates any optical evidence for the value of the B_{1u} mode ν_{13}.

With the new reassignments, the RMSΔ between the experimental and B3LYP/aug-cc-pVTZ results is reduced from 42 to 20 cm^{-1}. The largest remaining discrepancy is for ν_{14}, the B_{2u} mode calculated to be at 1298 cm^{-1} but placed at 1252 cm^{-1} on the basis of IR data. This is too high in frequency to have been observed in the INS spectrum, so its position remains uncertain.

The INS spectrum of TFB is compared with the calculated spectrum in Figure 2 and Table 2. The simulated spectra obtained from the sum of the squares of the hydrogen atom motions were superimposable for all five calculations of Table 2. The first point to note is that there is no intensity in the region just below 800 cm^{-1} where ν_{18} has been assigned. Further, the complex intensity in the region near 850 cm^{-1} appears to be well reproduced as a sum of the contributions from ν_{18} and ν_{15} which are both expected to be in this region. In this case the absence of any intensity from a band that is expected to be strong is deciding evidence that the value of the frequency of ν_{18} must be revised upward. The assignment for ν_6, an optically forbidden transition, has also been moved to higher frequency because there seems to be little intensity in the region of its original assignment (1165 cm^{-1}). These two changes significantly reduce the RMS deviation between experiment and calculation from 28 to 19 cm^{-1}.

Conclusions

In summary, on the basis of the above arguments in conjunction with the new INS data and the DFT results, we suggest the following reassignments for the fundamental vibrations of HFB: ν_5 (B_{2g}) = 205 cm^{-1}, ν_{15} (B_{2u}) = 278 cm^{-1}, ν_{13} (B_{1u}) = 600 cm^{-1}, and ν_3 (A_{2g}) = 788 cm^{-1}. For TFB, the proposed reassignments are ν_{18} (E'') = 852 cm^{-1} and ν_6 (A_2') = 1206 cm^{-1}. Fluorination of the benzene ring causes a decrease in the CC bond length. After the necessary corrections for vibrational effects, the B3LYP/aug-cc-pVTZ geometry for HFB is in good agreement with both the GED geometries and the experimental value of the rotational constant.

Acknowledgment. The Rutherford Appleton Laboratory is thanked for access to neutron beam facilities at ISIS. Stewart Parker of the ISIS facility is thanked for his expert assistance. Kenneth and Lise Hedberg are thanked for their provision of and assistance with the ASYM40 program. This work was partially supported by the U.S. National Science Foundation under grant CHE 9803058 and utilized the computer systems Exemplar and SGI PCarray at the National Center for Supercomputing Applications, University of Illinois at Urbana-Champaign.

References and Notes

(1) Scott, A. P.; Radom, L. *J. Phys. Chem.* **1996**, *100*, 16502−16513.
(2) Foley, M. S. C.; Braden, D. A.; Hudson, B. S.; Zgierski, M. Z. *J. Phys. Chem.* **1997**, *101*, 1455−1459.
(3) Dixon, D. A.; Feller, D.; Sandrone, G. *J. Phys. Chem. A* **1999**, *103*, 4744−4751.
(4) Dixon, D. A. *J. Phys. Chem.* **1986**, *90*, 2038−2043.
(5) Albinsson, B.; Michl, J. *J. Phys. Chem.* **1996**, *100*, 3418−3429.
(6) Röthlisberger, U.; Laasonen, K.; Klein, M. L.; Sprik, M. *J. Chem. Phys.* **1996**, *104*, 3692−3700.
(7) Papasavva, S.; Illinger, K. H.; Kenny, J. E. *J. Phys. Chem.* **1996**, *100*, 10100−10110.
(8) Baker, J.; Pulay, P. *J. Comput. Chem.* **1998**, *19*, 1187−1204.
(9) Green, J. H. S.; Harrison, D. J. *J. Chem. Thermodyn.* **1976**, *8*, 529−544.
(10) Laposa, J. D.; Montgomery, C. *Spectrochim. Acta A* **1982**, *38*, 1109−1113.
(11) Almlöf, J.; Faegri, K. *J. Chem. Phys.* **1983**, *79*, 2284−2294. Almlöf, J.; Faegri, K. *J. Am. Chem. Soc.* **1983**, *105*, 2965−2969.
(12) Thalladi, V. R.; Weiss, H.-G., Bläser, D.; Boese, R.; Nangia, A.; Desiraju, G. R. *J. Am. Chem. Soc.* **1998**, *120*, 8702−8710.
(13) Saebø, S.; Sellers, H. *J. Phys. Chem.* **1988**, *92*, 4266−4269.
(14) Gandhi, S. R.; Benzel, M. A.; Dykstra, C. E.; Fukunaga, T. *J. Phys. Chem.* **1982**, *86*, 3121−3126.
(15) Yokozeki, A.; Bauer, S. H. *Top. Curr. Chem.* **1975**, *53*, 71−119.
(16) Parker, S. F.; Carlile, C. J.; Pike, T.; Tomkinson, J.; Newport, R. J.; Andreani, C.; Ricci, F. P.; Sachetti, F.; Zoppi, M. *Physica B* **1998**, *154*, 241−243.
(17) Frisch, M.; Robb, M.; Cheeseman, J. R.; Stratmann, R.; Burant, J.; Dapprich, S.; Daniels, A.; Kudin, K.; Strain, M.; Farkas, O.; Barone, V.; Cossi, M.; Cammi, R.; Mennucci, B.; Pomelli, C.; Clifford, S.; Ochterski, J.; Petersson, G.; Ayala, P.; Cui, Q.; Morokuma, K.; Malick, D.; Rabuck, A.; Raghavachari, K.; Foresman, J.; Cioslowski, J.; Ortiz, J.; Stefanov, B.; Liu, G.; Liashenko, A.; Piskorz, P.; Komaromi, I.; Gomperts, R.; Martin, R.; Fox, D.; Keith, T.; Al-Laham, M.; Peng, C.; Nanayakkara, A.; Gonzalez, C.; Challacombe, M.; Gill, P. M. W.; Johnson, B.; Chen, W.; Wong, M.; Andres, J.; Gonzalez, C.; Head-Gordon, M.; Replogle, E.; Pople, J. *Gaussian 98*, Rev. A.6.; Gaussian, Inc.: Pittsburgh, 1998.

(18) Hudson, B. S.; Warshel, A.; Gordon, R. G. *J. Chem. Phys*. **1974**, *61*, 2929−2939.
(19) Zemach, A. C.; Glauber, R. J. *Phys. Rev*. **1956**, *101*, 118−129. Zemach, A. C.; Glauber, R. J. *Phys. Rev*. **1956**, *101*, 129−136.
(20) Korppi-Tommola, J.; Shurvell, H. F.; Daunt, S. J.; Steele, D. *J. Mol. Spectrosc*. **1981**, *87*, 382−392.
(21) Scherer, J. R.; Evans, J. C.; Muelder, W. W. *Spectrochim. Acta* **1962**, *18*, 1579−1592.
(22) Schlupf, J.; Weber, A. *J. Raman Spectrosc*. **1973**, *1*, 3−15.
(23) Mills, I. M. In *Molecular Spectroscopy: Modern Research*; Rao, K. N., Mathews, C. W., Eds.; Academic Press: New York, 1972. Papousek, D.; Aliev, M. R. *Molecular Vibrational−Rotational Spectra*; Elsevier: Amsterdam, 1982.
(24) Hedberg, L.; Mills, I. M. *J. Mol. Spectrosc*. **1993**, *160*, 117−142.
(25) Langseth, A.; Stoicheff, B. P. *Can. J. Phys*. **1956**, *34*, 350−353.
(26) Carlos, J. L., Jr.; Karl, R. R., Jr.; Bauer, S. H. *J. Chem. Soc., Faraday Trans. 2*, **1974**, *21*, 177−187.
(27) Bent, H. A. *Chem. Rev*. **1961**, *61*, 275−311.
(28) Almenningen, A.; Bastiansen, O.; Seip, R.; Seip, H. M. *Acta Chem. Scand*. **1964**, *18*, 2115−2124.
(29) Berry, R. J.; Burgess, D. R. F., Jr.; Nyden, M. R.; Zachariah, M. R.; Schwartz, M. *J. Phys. Chem*. **1995**, *99*, 17145−17150.
(30) Guo, H.; Karplus, M. *J. Phys. Chem*. **1992**, *96*, 7273−7287.
(31) Steele, D.; Whiffen, D. H. *Trans. Faraday Soc*. **1959**, *55*, 369−376.
(32) Boden, N.; Davis, P. P.; Stam, C. G.; Wesselink, G. A. *Mol. Phys*. **1973**, *25*, 81−86. Bertolucci, M. D.; Marsh, R. E. *J. Appl. Crystallogr*. **1974**, *7*, 87−88.
(33) Bauer, S. H.; Katada, K.; Kimura, K. In *Structural Chemistry and Molecular Biology*; Rich, A., Davidson, N., Eds.; W. H. Freeman: San Francisco, 1968.